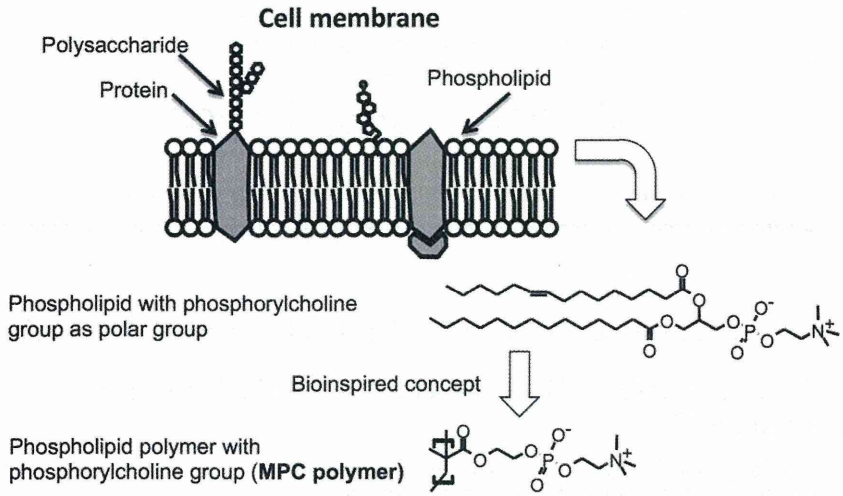

Fig. 1. Schematic representation of cell membrane.

functions. Numerous biomolecules are embedded in the phospholipid bilayer, e.g., antibodies, glycoproteins, enzymes, and receptors. The favorable biofunctions are inertness of the capsule, biological affinity, enzymatic reaction, etc. These are fundamental biomolecules that play important roles. In the bioinspired approach, molecular components were assembled to perform these selected biofunctions. For example, phospholipids comprise a polar head group and alkyl tail groups. However, surface enrichment of phospholipid polar groups is essential for preparing the biointerface. In other words, the entire phospholipid molecules are not necessary for formation of the biointerface. This is the concept of a fundamental bioinspired approach; we introduce polymer materials to prepare the stable biointerface.

The requirements of establishing ultimate biointerfaces are (i) bioinertness, (ii) easy fabrication, (iii) immobilization of biomolecules under mild condition, (iv) retention of higher biofunctions, and (v) easy accessibility of target molecules without any barrier. We have been utilizing polymers composed of 2-methacryloyloxyethyl phosphorylcholine (MPC), which has phosphorylcholine group in the side chain, as a key material for constructing a biointerface platform. Very recently, some researchers utilized other methacrylates with zwitter ionic polar groups or oligo(ethylene glychol) monomethacrylate for preparing biointerfaces to obtain low fouling surfaces [24–29].

2.2. Biointerfaces composed of the MPC polymers

The biointerface researches with MPC polymers have been conducted worldwide [30–33]. It has opened up new avenues for investigation, particularly in the field of life science research. The MPC allows versatile polymerization techniques with appropriate comonomers: conventional radical, living radical and atom transfer radical polymerizations. Therefore, precisely designed MPC polymers have been easily synthesized; herein, the ultimate biointerfaces by the MPC polymer is introduced along with recent excellent results. The synthesized MPC polymers are used in various forms such as polymer solution, hydrogel, polymer-coated surface, polymer-grafted surface, and nanoparticles. In particular, hydrophilic MPC unit and hydrophobic *n*-butyl methacrylate (BMA) unit are of great importance for the fabrication of high-performance biointerfaces. The best monomer unit fraction in the copolymer for coating on the medical devices was reported to be 0.3 of the MPC unit and 0.7 of the BMA unit; moreover, the molecular weight of the copolymer should be controlled to above 5×10^5 [9,11]. The MPC polymer-coated surface serves double functions—suppression of nonspecific protein adsorption from the living organism and processing of robust polymer coating. On the surface treated with the MPC polymer, the phosphorylcholine groups in the MPC unit were enriched in the outermost surface of the substrate relative to the inner side of the substrate [34,35]. The plausible mechanism for the suppression of nonspecific protein adsorption was discussed in terms of water structure on the surface. Enrichment of the phosphorylcholine groups provided a higher free water fraction on the polymer-coated surface, and it strongly suppressed protein adsorption by release of bound water molecules on the protein surface. [36–39].

Based on the chemical structure of the poly(MPC-*co*-BMA), which provides excellent anti-biofouling surface, the new polymers are designed to conjugate biomolecules on the surface under mild conditions. The reaction for conjugation of biomolecules must be carried out in an aqueous medium with physiological pH range and temperature due to low stability of biomolecules. So, active ester groups and phenylboronic acid group are useful for reacting with amino group and sugar units in the biomolecules, respectively.

As shown in Fig. 2, a polymer composed of MPC, BMA, and *p*-nitrophenyloxycarbonyl poly(oxyethylene)methacrylate (MEONP) units (the polymer is named as PMBN) was designed and prepared for obtaining excellent biointerfaces [40,41]. These three monomer units show unique chemical and biological functions. One of the bioconjugate functions was the incorporation of an active ester group on MEONP. The active ester group was connected to the methacrylate via the oxyethylene spacer [42]. The length of the oxyethylene spacer can be changed with the use of appropriate precursors. The spacer length was changed from 0.5 to 2 nm, and the location of the immobilized biomolecules was also changed. The phosphorylcholine groups were at the position of 0.4 nm from the substrate, which was calculated by the molecular structure of the MPC unit. We found that the durability of the immobilized biomolecules depended on the spacer length, by changing the number of repeating units of the oxyethylene group in MEONP. The spacer length played a key role in reducing background signals in γ-globulin (IgG)-immobilized biosensing. Biomolecules containing amino groups could couple to the ester groups on the polymer backbone under physiological conditions, producing *p*-nitrophenol as a leaving group. The bioconjugate reaction is accelerated under neutral or weak alkaline conditions (pH 7.4–8.0). By this polymer, PMBN, the biomolecules could immobilize in the platform of phosphorylcholine group-enriched surface the same as cell membrane surfaces. Also, it could be prepared from nano-scaled structure using PMBN on the surface of electrode by electrospray deposition (ESD) method to enlarge surface area for conjugation of biomolecules. Much amount of biomolecules could be immobilized on the ESD-surface compared with that on plane spin-coated surface [43].

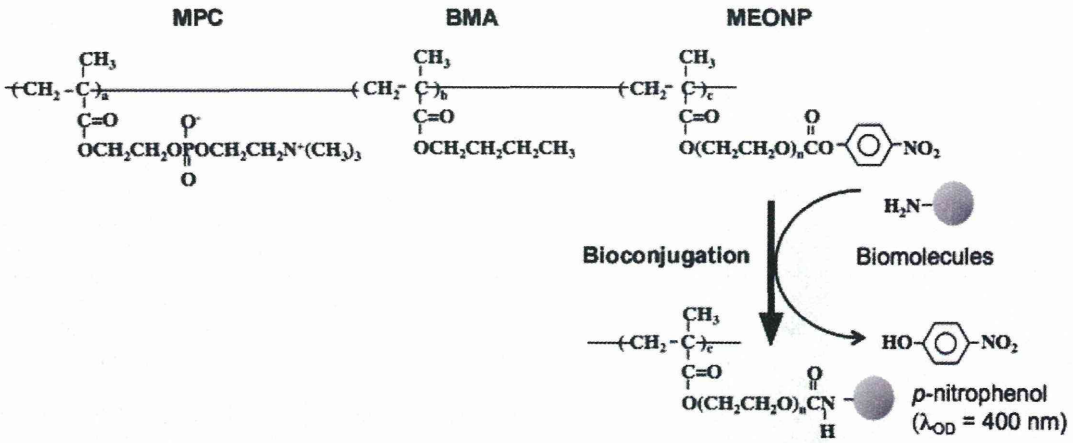

Fig. 2. Chemical structure of phospholipid polymer, poly(MPC-*co*-BMA-*co*-MEONP) (PMBN) for bioconjugation based on artificial membrane structure.

3. Polymer nanoparticles with artificial cell membrane surface

3.1. Preparation of polymer nanoparticles

We focus on monodispersed nanoparticles as one of the biointerfaces, and introduce affinity separation, sensing, and diagnosis. The PMBN was easily enriched onto the nanoparticle surface by the solvent evaporation method. We first succeeded in preparing monodispersed nanoparticles covered with water-soluble and amphiphilic poly(MPC-*co*-BMA) (PMB30W: mole fraction of MPC unit in the polymer is 0.30). The PMB30W aqueous solution provided hydrophobic domains by aggregation of the polymer chain [44]. This is the fundamental driving force for the reduction of surface free energy (water–methylene chloride interface) to stabilize methylene chloride droplets involved in the formation of other polymers such as poly(lactic acid) (PLA) and polystyrene. Moreover, Konno et al. first developed monodispersed PLA nanoparticles covered with PMBN (PMBN/PLA-NP) [45]. The phosphorylcholine groups in the MPC unit and active ester groups in the MEONP groups were enriched in the outermost surface; evidence for this was obtained by X-ray photoelectron spectroscopy. The average diameters of the PMBN/PLA-NP ranged from 250 nm to 300 nm as shown in Fig. 3. The zeta-potential of the PLA surface was a large negative value about −60 mV, however, that of the PMBN/PLA-NP became to ranged from −6.8 mV to −2.0 mV. This is because of the electrical neutrality of the phosphorylcholine groups due to the formation of an inner salt between phosphate anions and trimethylammonium cations. The appropriate materials that can be used as nanoparticle cores are polymers, metals, and ceramic. In particular, PMBN enables coating of the particle surface; thus, titanium oxide and silica nanoparticles are easily coated by PMBN. Active ester groups were located on the nanoparticles, and the typical surface concentration was evaluated to be 1.0 nmol per mg of polystyrene nanoparticles (PS-NP). The bioconjugation was achieved simultaneously as well as continuously. Moreover, multiple biomolecules could be immobilized via the active ester groups [46–48]. We observed that multiple immobilizations of proteins on the PMBN-coated nanoparticles were achieved. Considering this, PMBN comprising phosphorylcholine and active ester groups is of great importance as a platform for a high-performance biointerface facilitating affinity separation, sequential reaction, and biomolecular detection.

3.2. Binding of target biomolecules on nanoparticles based on bioreaction

Nonselective adsorption of biomolecules on the surface makes noise for sensing of target molecules. The MPC polymer can suppress protein adsorption significantly. The effects of the phosphorylcholine groups on the adsorption of bovine serum albumin (BSA) to the nanoparticles were evaluated [49]. To avoid chemical reaction with BSA, the active ester groups on PMBN/PLA-NP were reacted with glycine for blocking the active ester groups in this experiment. Fig. 4

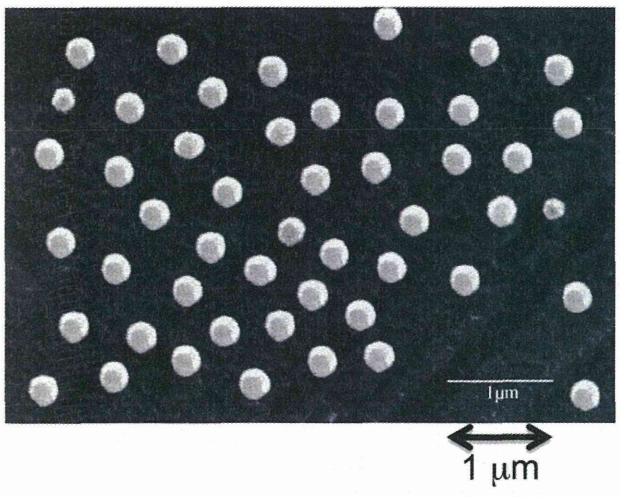

Fig. 3. Electron microscopic picture of polymer nanoparticles covered with artificial cell membrane.

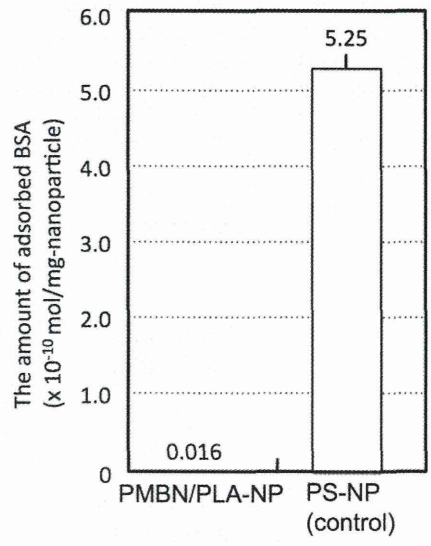

Fig. 4. Amount of BSA adsorbed on polymer nanoparticles without and with artificial cell membrane surface.

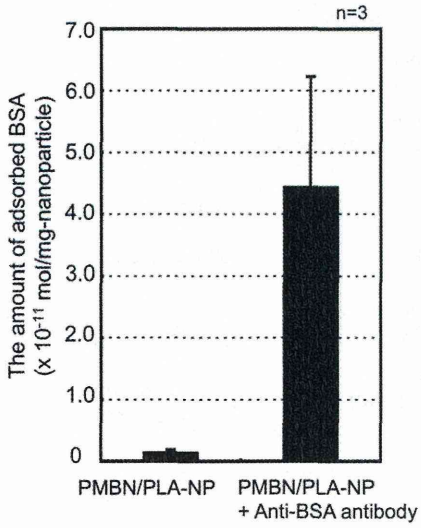

Fig. 5. Amount of BSA captured on polymer nanoparticles immobilized anti-BSA antibody based on antigen–antibody reaction.

shows the amount of BSA adsorbed on various nanoparticles. Numerous BSA molecules were adsorbed on the commercially available PS-NP whereas these molecules were hardly adsorbed on the glycine-reacted PMBN/PLA-NP; the value was approximately 1/300 as compared with that on PS-NP. The surface of PS-NP was hydrophobic and adsorbed proteins. PMBN/PLA-NP was suitable for developing affinity nanoparticles because of their considerable ability to prevent nonspecific adsorption.

The activity and function of the antibody immobilized on the PMBN/PLA-NP were evaluated by observing the antigen–antibody reaction (Fig. 5). The amount of BSA on the anti-BSA antibody-immobilized PMBN/PLA-NP was higher than that on PMBN/PLA-NP without antibody immobilization. This result indicates that the amount of BSA increased by reacting with the antibody immobilized on the surface of PMBN/PLA-NP. Based on this result, the antibody-immobilized PMBN/PLA-NP could function as affinity nanoparticles. The dissociation constant (Kd) of the antigen/antibody complex substantially defines the performance of affinity-based separation, diagnosis, and detection systems. To evaluate the performance of PMBN/PLA-NP as an affinity nanoparticle, the dissociation constant of the antigen/antibody complex on PMBN/PLA-NP was measured [49]. The dissociation constant could be calculated from these plots, and it was observed to be 2.7×10^{-7} M for the anti-BSA antibody-immobilized PMBN/PLA-NP (PMBN/PLA/anti-BSA-NP) and 1.3×10^{-5} M for the anti-BSA antibody-immobilized PS-NP modified with succinimide moiety (PS-suc-NP) on the surface (PS/anti-BSA-NP). Thus, the affinity of the anti-BSA antibody to BSA observed on the PMBN/PLA/anti-BSA-NP was approximately 200-fold higher than that on the PS/anti-BSA-NP. The K_d value generally ranges from 10^{-7} to 10^{-10} for an antigen–antibody complex [50]. The K_d value of the anti-BSA antibody immobilized on PMBN/PLA-NP for BSA is considered valid while that for the anti-BSA antibody immobilized on PS-suc-NP is higher than the reported value. This indicates that the antibody immobilized on the PMBN/PLA-NP had a strong affinity toward the antigen, maintaining the activity of the antibody even when immobilized on the nanoparticles. However, in the case of antibodies immobilized on the PS-suc-NP, a large K_d value was observed; this was due to a weakening in the affinity for the antigen by denaturation of the antibody during immobilization. These results indicate the effects of the phosphorylcholine groups in preventing the denaturation of the antibody.

4. Specific cellular uptake of nanoparticles covered with artificial cell membrane conjugated with specific biomolecules

4.1. Preparation of polymer nanoparticles embedding fluorescence marker

Semiconductor nanocrystalites (quantum dots or QDs) have gained much interest as a promising alternative to organic dyes for biological imaging. QDs ranging in size between 2 nm and 6 nm have unique optical properties: material- and size-dependent emission spectra, a wide absorption spectrum, high quantum yields, simultaneous multicolor emissions, and especially excellent resistance to photobleaching. This photostability is a critical feature in most fluorescence applications, particularly for long-term monitoring of labeled substances, and is an area in which QDs have a singular advantage over organic dyes. As QDs themselves are hydrophobic, the key to developing QDs as a tool in biological systems is to achieve good dispersion ability in an aqueous medium, and compatibility with biological components including cells [51–53].

Polymer nanoparticles embedding QDs covered with PMBN (PMBN/PLA/QD) were designed by making an assembly of phosphorylcholine groups as platform and biomolecules immobilized on the surface of nanoparticles (Fig. 6) [54]. In spite of numerous efforts [55,56], the problems of cytotoxicity and the nonselective cellular uptake of QDs remain. As mentioned above, the PMBN/PLA-NPs show the bioinert abilities and they may avoid phagocytosis from macrophage-like cells [57]. That is, the phosphorylcholine group coverings suppress nonspecific interactions between bulk materials and cell, and create a specific affinity by ligand molecules immobilized on the surface.

4.2. Cellular uptake of the PMBN/PLA/QD

We observed that PMBN/PLA/QD had the abilities to highly resist nonselective cellular uptake from HeLa cells and to permeate the membrane of HeLa cells effectively when arginine octapeptide (R8)

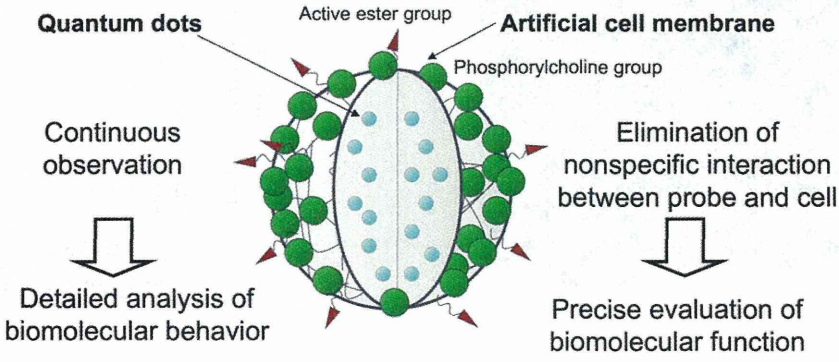

Fig. 6. Schematic representation of polymer nanoparticles embedding QD with artificial cell membrane surface.

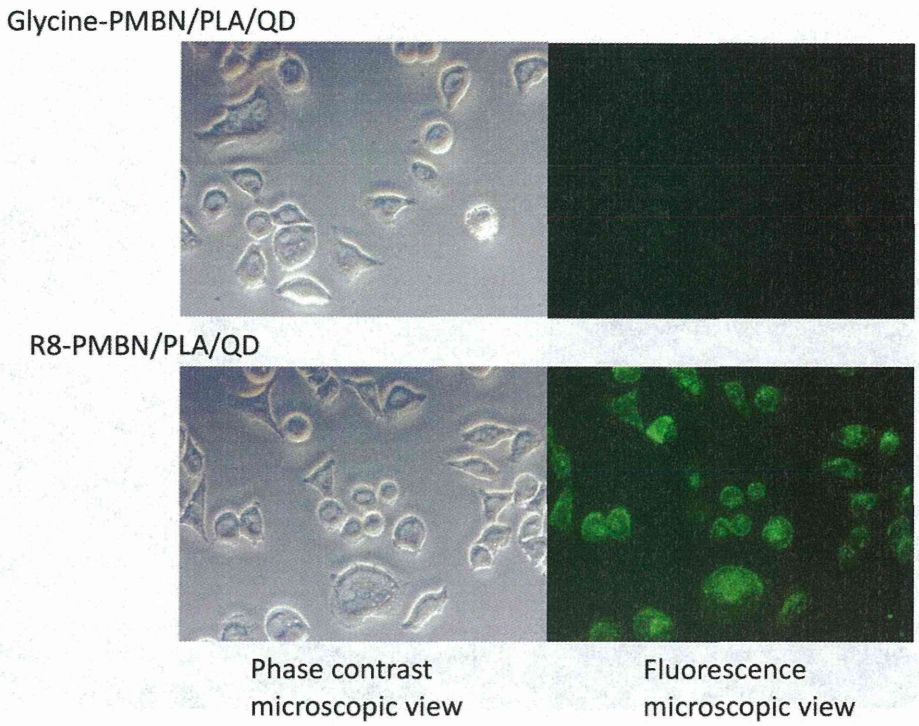

Fig. 7. Uptake of polymer nanoparticles covered with artificial cell membrane without and with R8 immobilization.

was immobilized on the surface of the nanoparticles as shown in Fig. 7 [54]. The R8 is well known as cell membrane penetrating peptide (CPP), so its specific functions are observed with the polymer nanoparticles. In Fig. 8, a plot of the intensity of each PMBN/PLA/QD in cells versus incubation time shows that glycine-masked PMBN/PLA/QD (glycine–PMBN/PLA/QD) completely suppresses the nonselective uptake from HeLa cells. We also confirmed that no glycine–PMBN/PLA/QD was uptaken by HeLa cell even after incubation for 24 h. In general, conventional nanoparticles can be uptaken by the cells without any selectively [57]. Thus, this result indicated that our PMBN/PLA/QD can obtain high signal to noise ratio compared with other imaging probes because there is no background fluorescence caused by nonselective uptake of imaging probes. On the other hand, R8-conjugated PMBN/PLA/QD internalized effectively into cells. The uptake of R8–PMBN/PLA/QD significantly increased within first 15 min, but the uptake rate gradually slowed and reached a plateau at 1 h. However, we cannot obtain from only this information where R8–PMBN/PLA/QD located in the cell at each time. Thus, further research about the location of R8–PMBN/PLA/QD was required.

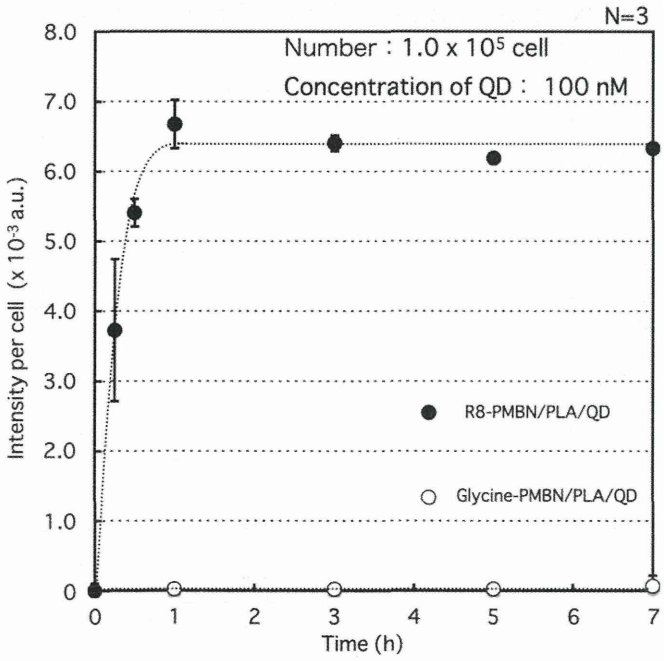

Fig. 8. Time dependence of cellular uptake of polymer nanoparticles. Closed plots: glycine–PMBN/PLA/QD, open plots: R8–PMBN/PLA/QD.

For determining the location of R8–PMBN/PLA/QD at each time, HeLa cells incubated with R8–PMBN/PLA/QD was observed by a confocal laser scanning microscopy (CLSM). Fig. 9 shows that R8–PMBN/PLA/QD attached immediately to the cell membrane within first 5 min and began to internalize into endosome at 15–30 min. The amount of internalized R8–PMBN/PLA/QD increased at 1–3 h and whole R8–PMBN/PLA/QD which attached to cell membrane entered into endosome in 5 h. These results revealed the kinetic behavior of R8-mediated internalization into the cell. Several lines of evidences demonstrated that the PMBN/PLA/QD is a most suitable analytic tool for kinetic analysis of biomolecules.

4.3. The evaluation of the inflammatory response induced by PMBN/PLA/QD

It was reported that PMBN/PLA/QD have no cytotoxicity for 3 days even after internalization in HeLa cells [51]. However, there are some possibilities of the induction of inflammation reaction even when no cytotoxicity appears. Thus, more studies are required with respect to the inflammatory response.

Mouse macrophage RAW264.7 cell, known for its sensitivity to inflammatory response, was used as a model system. RAW264.7 cell was incubated with PMBN/PLA/QD for 24 h. After incubation, the inflammatory response was measured by using real-time reverse transcription polymerase chain reaction (RT-PCR). Oligonucleotides TNF-α-F (5′-GAGCAGCTGGAGTGGCTGCTGAG-3′) and TNF-α-R (5′-

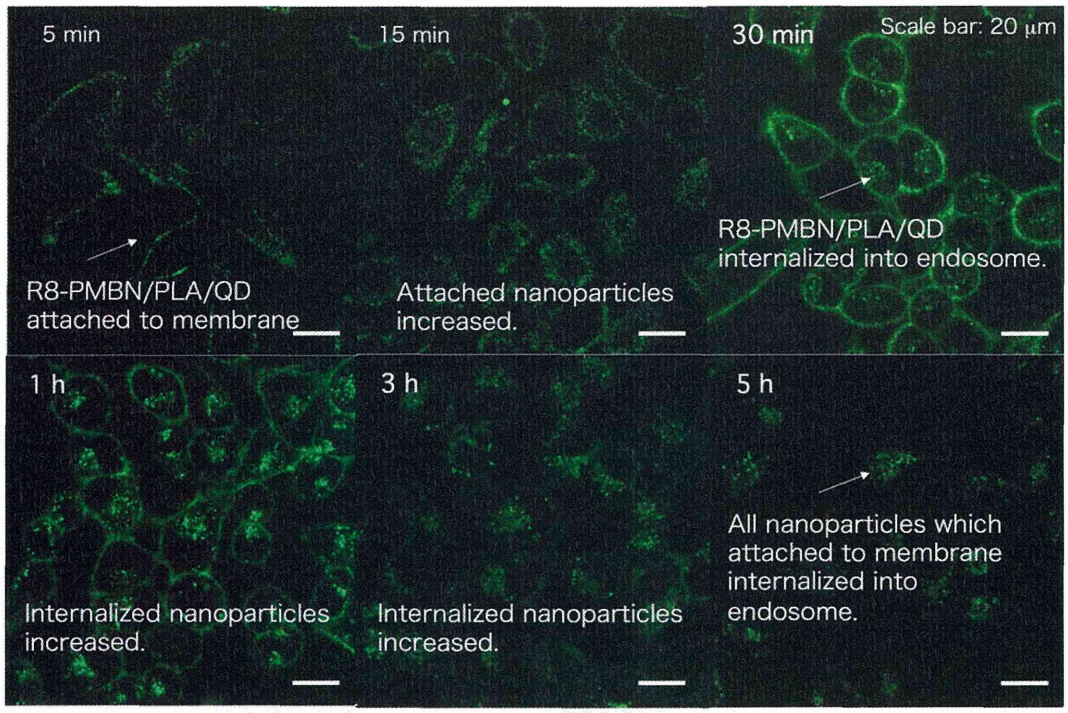

Fig. 9. LCMS analysis of internalization of R8–PMBN/PLA/QD.

TAGACCTGCCCGGACTCCGC-3′) were used for detection of tumor necrosis factor-alpha (TNF-α); GAPDH-F (5′-AATGTGTCCGTCGTGGAT CT-3′) and GAPDH-R (5′-CCCTGTTGCTGTAGCCG TAT-3′) were used for glyceraldehydes-3-phosphate dehydrogenase (GAPDH). The expression of TNF-α mRNA was standardized as the relative value to that obtained for GAPDH mRNA. As negative and positive controls, a normal cell and the cell with 100 ng/mL lipopolysaccharide were used respectively. Fig. 10 shows the relative expression of TNF-α mRNA to GAPDH mRNA in RAW264.7 cells incubated with R8 or glycine–PMBN/PLA/QD for a day. No significant difference between negative control and PMBN/PLA/QDs in the expression of TNF-α mRNA was observed. This indicated that phosphorylcholine groups on the surface of PMBN/PLA/QD suppress the inflammatory reaction in RAW264.7 cells even when internalizing into cells due to the ologopeptide. From these findings, our PMBN/PLA/QD can eliminate the unwished interactions between probes themselves and cell, such as a nonselective cellular uptake, cytotoxicity and inflammation response.

4.4. The assessment of the abilities of various octapeptides as a cell membrane penetration peptide

Many research groups reported that arginine-rich peptide is useful as a CPP [58,59]. However, the abilities of other oligopeptides to penetrate the cell membrane have not been well characterized. Thus, we evaluated the function of various octapeptides as a CPP by using our PMBN/PLA/QD as an analyzing tool. To assess the main factor

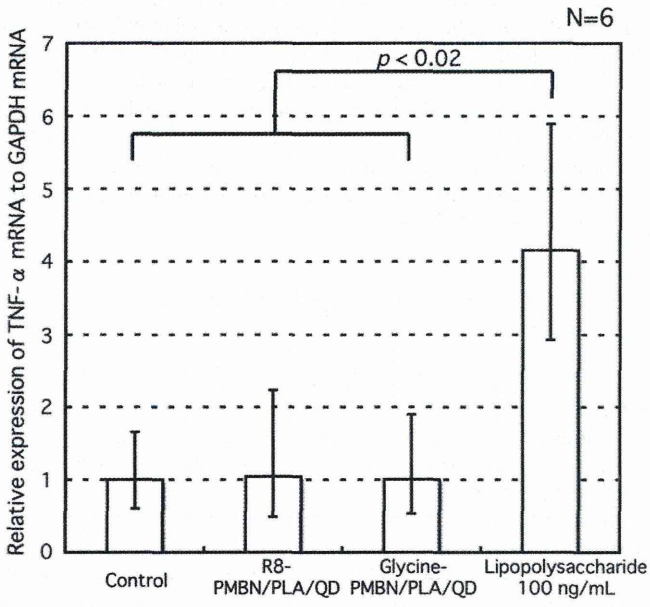

Fig. 10. Relative expression of TNF-α mRNA to GAPDH mRNA in RAW264.7 cells incubated with polymer nanoparticles.

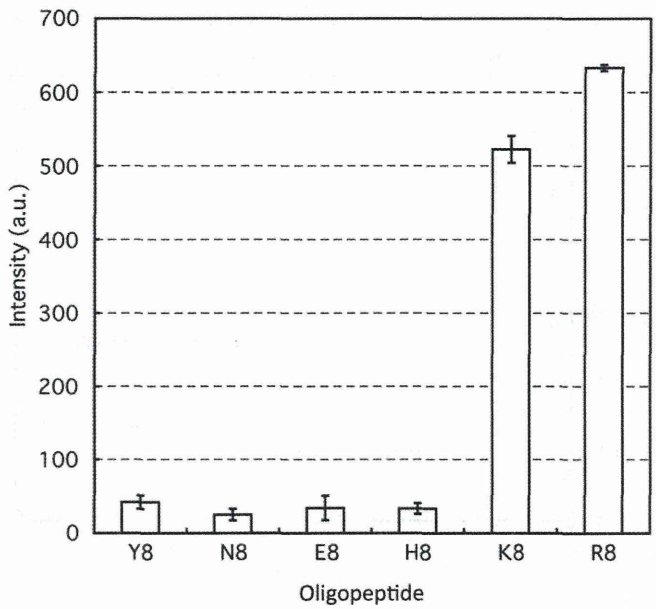

Fig. 11. Effect of amino acid residue of immobilized oligopeptide on cellular uptake.

determining the abilities of oligopeptides as a CPP, we selected various octapeptides that consist of one kind of amino acid (octa-tyrosine (Y8: hydrophobic), octa-asparagine (N8: hydrophilic), octa-glutamic acid (E8: hydrophilic and anionic), octa-histidine (H8: hydrophilic and weakly cationic), octa-lysine (K8: hydrophilic and cationic), or octa-arginine (R8: hydrophobic and cationic)). These peptides were conjugated with PMBN/PLA/QD respectively. A HeLa cell (seeded into 12-well plates at 1.0×10^4 cell/well in 1 mL of culture medium) was incubated with each octapeptide-conjugated PMBN/PLA/QD for 5 h. The quantification of the uptake of PMBN/PLA/QD was performed. As shown in Fig. 11, only K8 and R8 conjugated PMBN/PLA/QD could internalize in HeLa cells. This result indicated that the hydrophilic and cationic nature of oligopeptides play a key role in the cell membrane permeation. In order to understand the mechanism of cell penetration induced by these hydrophilic and cationic oligopeptides, it will be required to investigate the relationship between surface cationic density on the nanoparticles and cell membrane permeation.

5. Conclusion

Many important applications of nanotechnology would not be achievable without proper design of nanosturcture. As integrative field of biomedical nanotechnology evolves, more systematic approaches for the chemical design of nanostructures will be required. Furthermore, as the researchers start to construct multifunctional nanostructures, the interface between nanostructure and biological environments will be critical. In this study, our artificial cell membrane–biointerface can provide the imaging probes with the abilities to suppress completely the interactions between imaging probes themselves and cells. This biointerface is necessary to study the fundamental information of the biomolecular behavior in cellular environments. We described the kinetic behavior in cytoplasm of our polymer nanoparticles containing QDs with artificial cell membrane–biointerface. Although these nanoparticles can avoid the nonselective cellular uptake from mammalian cells, when bioactive molecules were immobilized, our nanoparticles can provide the various information about the specific interaction between biomolecules and cells. From these findings, we conclude that the nanoparticles are candidates for the role of stable and highly sensitive fluorescent bioimaging probes in the fields of nanotechnology. Controlling interactions with cells is receiving considerable importance in biomedical fields, including nanobioengineering and cell and tissue engineering. The bioinspired interfaces described here are a promising design for revealing a universal platform that integrates polymer chemistry; material science; and engineering, biochemistry, cell biology, and nanofabrication.

Acknowledgements

This research was partially supported by Special Coordination Funds for Promoting Science and Technology from the Ministry of Education, Culture, Sports, Science, and Technology, Japan.

References

[1] S.J. Singer, G.L. Nicholson, The fluid mosaic model of the structure of cell membranes, Science 175 (1972) 720–731.
[2] P.L. Yeagle, The Membranes of Cells, second ed.Academic Press, New York, 1993.
[3] J.A. Hayward, D. Chapman, Biomembrane surfaces as models for polymer design: the potential for haemocompatibility, Biomaterials 5 (1984) 135–142.
[4] J.J. Ramsden, G.I. Bachmanova, A.I. Archakov, Immobilization of proteins to lipid bilayers, Biosens. Bioelectron. 5 (1996) 523–528.
[5] X.L. Sun, W. Cui, T. Kai, E.L. Chaikof, A facile synthesis of bifunctional phospholipids for biomimetic membrane engineering, Tetrahedron 60 (2004) 11765–11770.
[6] L. Brunsveld, H. Waldmann, D. Huster, Membrane binding of lipidated Ras peptides and proteins—the structural point of view, Biochim. Biophys. Acta 1788 (2009) 273–288.
[7] H.M. Cho, D.Y. Cho, J.Y. Jeon, S.Y. Hwang, I.S. Ahn, J. Choo, E.K. Lee, Fabrication of protein-anchoring surface by modification of SiO_2 with liposomal bilayer, Colloids Surf. B: Biointerfaces 75 (2010) 209–213.
[8] K. Ishihara, J. Watanabe, Y. Iwasaki, Bioinspired polymer surfaces for prevention of bioresponse, Mater. Sci. Forum 426–432 (2003) 3171–3176.
[9] J. Watanabe, J.-W. Park, T. Ito, M. Takai, K. Ishihara, Biofunctionalization of phospholipid polymer nanoparticles, in: C.S.S.R. Kumar (Ed.), Nanotechnologies for the Life Science, Biofunctionalizaation of Nanomaterials, vol. 1, Wiley-VCH, Weinheim, 2005, pp. 125–149.
[10] J. Watanabe, K. Ishihara, Biointerface, bioconjugation, and biomatrix based on bioinspired phospholipid polymers, in: H.S. Nalwa (Ed.), Handbook of Nanostructured Biomaterials and Their Applications in Nanobiotechnology vol. 1, American Scientific Publishers, 2005, pp. 129–165.
[11] J. Watanabe, K. Ishihara, Establishing ultimate biointerfaces covered with phosphorylcholine groups, Colloids Surf. B: Biointerfaces 65 (2008) 155–165.
[12] K. Ishihara, K. Nishizawa, Y. Goto, M. Takai, Bioinspired polymer surfaces for nanodevices and nanomedicine, Adv. Sci. Technol. 57 (2008) 5–14.
[13] K. Ishihara, T. Ueda, N. Nakabayashi, Preparation of phospholipid polymers and their properties as polymer hydrogel membrane, Polym. J. 22 (1990) 355–360.
[14] T. Ueda, H. Oshida, K. Kurita, K. Ishihara, N. Nakabayashi, Preparation of 2-methacryloyloxyethyl phosphorylcholine copolymers with alkyl methacrylates and their blood compatibility, Polym. J. 24 (1992) 1259–1269.
[15] K. Ishihara, R. Aragaki, T. Ueda, A. Watanabe, N. Nakabayashi, Reduced thrombogenicity of polymers having phospholipid polar groups, J. Biomed. Mater. Res. 24 (1990) 1069–1077.
[16] K. Ishihara, N.P. Ziats, B.P. Tierney, N. Nakabayashi, J.M. Anderson, Protein adsorption from human plasma is reduced on phospholipid polymers, J. Biomed. Mater. Res. 25 (1991) 1397–1407.
[17] K. Ishihara, H. Oshida, Y. Endo, T. Ueda, A. Watanabe, N. Nakabayashi, Hemocompatibility of human whole blood on polymers with a phospholipid polar group and its mechanism, J. Biomed. Mater. Res. 26 (1992) 1543–1552.
[18] T.A. Snyder, H. Tsukui, S. Kihara, T. Akimoto, K.N. Litwak, M.V. Kameneva, Preclinical biocompatibility assessment of the EVAHEART ventricular assist device: coating comparison and platelet activation, J. Biomed. Mater. Res. A 81 (2007) 85–92.
[19] G.J. Myers, D.R. Johnstone, W.J. Swyer, S. McTeer, S.L. Maxwell, C. Squires, S.N. Ditmore, C.V. Power, L.B. Mitchell, J.E. Ditmore, L.D. Aniuk, G.M. Hirsch, K.J. Buth, Evaluation of mimesys phosphorylcholine (PC)-coated oxygenators during cardiopulmonary bypass in adults, J. Extra-Corpor. Technol. 35 (2003) 6–12.
[20] M. Kyomoto, T. Moro, T. Konno, H. Takadama, N. Yamawaki, H. Kawaguchi, Y. Takatori, K. Nakamura, K. Ishihara, Enhanced wear resistance of modified cross-linked polyethylene by grafting with poly(2-methacryloyloxyethyl phosphorylcholine), J. Biomed. Mater. Res. A 82A (2007) 10–17.
[21] A.L. Lewis, L.A. Tolhurst, P.W. Stratford, Analysis of a phosphorylchline-based polymer coating on a coronary stent pre- and post-implantation, Biomaterials 23 (2002) 1697–1706.
[22] K. Ishihara, M. Takai, Bioinspired interfaces for nanobiodevices based on phospholipid polymer chemistry, J. R. Soc. Interface 6 (2009) S279–S291.
[23] K. Nishizawa, T. Konno, M. Takai, K. Ishihara, Bioconjugated phospholipid polymer biointerface for ELISA, Biomacromolecules 9 (2008) 403–407.
[24] E. Kharlampieva, D. Pristinski, S.A. Sukhishvili, Hydrogen-bonded multilayers of poly(carboxybetaine)s, Macromolecules 40 (2007) 6967–6972.
[25] Y. Chang, S.-C. Liao, A. Higuchi, R.-C. Ruaan, C.-W. Chu, W.-Y. Chen, A highly stable nonbiofouling surface with well-packed grafted zwitterionic polysulfobetaine for plasma protein repulsion, Langmuir 24 (2008) 5453–5458.
[26] Y.-C. Chianga, Y. Changb, A. Higuchia, W.-Y. Chena, R.-C. Ruaana, Sulfobetaine-grafted poly(vinylidene fluoride) ultrafiltration membranes exhibit excellent antifouling property, J. Membr. Sci. 339 (2009) 151–159.
[27] H. Vaisocherová, W. Yang, Z. Zhang, Z. Cao, G. Cheng, M. Piliarik, J. Homola, S. Jiang, Ultralow fouling and functionalizable surface chemistry based on a zwitterionic polymer enabling sensitive and specific protein detection in undiluted blood plasma, Anal. Chem. 80 (2008) 7894–7901.
[28] G. Cheng, G. Li, H. Xue, S. Chen, J.D. Bryers, S. Jiang, Zwitterionic carboxybetaine polymer surfaces and their resistance to long-term biofilm formation, Biomaterials 30 (2009) 5234–5240.
[29] S. Tugulu, H.-A. KlokStability, Nonfouling properties of poly(poly(ethylene glycol) methacrylate) brushes under cell culture conditions, Biomacromolecules 9 (2008) 906–912.
[30] X.-D. Huang, K. Yao, H. Zhang, X.-J. Huang, Z.-K. Xu, Surface modification of silicone intraocular lens by 2-methacryloyloxyethyl phosphoryl-choline binding to reduce *Staphylococcus epidermidis* adherence, Clin. Exp. Ophthalmol. 35 (2007) 462–467.
[31] W. Feng, S. Zhu, K. Ishihara, J.L. Brash, Adsorption of fibrinogen and lysozyme on silicon grafted with, poly(2-methacryloyloxyethyl phosphorylcholine) via surface-initiated atom transfer, radical polymerization, Langmuir 21 (2005) 5980–5987.
[32] S.F. Rose, S. Okere, G.W. Hanlon, A.W. Lloyd, A.L. Lewis, Bacterial adhesion to phosphorylcholine-based polymers with varying cationic charge and the effect of heparin pre-adsorption, J. Mater. Sci. Mater. Med. 16 (2005) 1003–1015.
[33] J.-J. Yuan, A. Schmid, S.P. Armes, Facile synthesis of highly biocompatible poly(2-(methacryloyloxy)ethyl phosphorylcholine)-coated gold nanoparticles in aqueous solution, Langmuir 22 (2006) 11022–11027.
[34] T. Ueda, K. Ishihara, N. Nakabayashi, Adsorption–desorption of proteins on phospholipid polymer surfaces evaluated by dynamic contact angle measurement, J. Biomed. Mater Res. 29 (1995) 381–387.
[35] A. Yamasaki, Y. Imamura, K. Kurita, Y. Iwasaki, N. Nakabayashi, K. Ishihara, Surface mobility of polymers having phosphorylcholine groups connected with various

bridging units and their protein adsorption-resistant properties, Colloids Surf. B: Biointerfaces 28 (2003) 53–62.
[36] K. Ishihara, H. Nomura, T. Mihara, K. Kurita, Y. Iwasaki, N. Nakabayashi, Why do phospholipid polymer reduce protein adsorption? J. Biomed. Mater. Res. 39 (1998) 323–330.
[37] T. Morisaku, J. Watanabe, T. Konno, M. Takai, K. Ishihara, Hydration of phosphorylcholine groups attached to highly swollen polymer hydrogels studied by thermal analysis, Polymer 49 (2008) 4652–4657.
[38] H. Kitano, M. Imai, T. Mori, M. Gemmei-Ide, Y. Yokoyama, K. Ishihara, Structure of water in the vicinity of phospholipid analog copolymers as studied by vibrational spectroscopy, Langmuir 19 (2003) 10260–10266.
[39] D.R. Lu, S.J. Lee, K. Park, Calculation of solvetion interaction energies for protein adsorption on polymer surface, J. Biomater. Sci. Polym. Edn. 3 (1991) 127–147.
[40] K. Takei, K. Konno, J. Watanabe, K. Ishihara, Regulation of enzyme–substrate complexation by phospholipid polymer conjugates for cell engineering, Biomacromolecules 5 (2004) 858–862.
[41] K. Kinoshita, K. Fujimoto, T. Yakabe, S. Saito, Y. Hamaguchi, T. Kikuchi, K. Nonaka, S. Murata, D. Masuda, W. Takada, S. Funaoka, S. Arai, H. Nakanishi, K. Yokoyama, K. Fujiwara, K. Matsubara, Multiple primer extension by DNA polymerase on a novel plastic DNA array coated with a biocompatible polymer, Nucleic Acids Res. 35 (e3) (2007) 1–9.
[42] J. Watanabe, K. Ishihara, Multiple protein immobilized phospholipid polymer nanoparticles: effect of spacer length on residual enzymatic activity and molecular diagnosis, Nanobiotechnology 3 (2008) 76–82.
[43] K. Nishizawa, M. Takai, K. Ishihara, Stabilization of phospholipid polymer surface with three-dimensional; nanometer-scales structure for highly sensitive immunoassay, Colloids Surf. B: Biointerfaces 77 (2010) 263–269.
[44] K. Ishihara, Y. Iwasaki, N. Nakabayashi, Polymeric lipid nanosphere constituted of poly(2-methacryloyloxyethyl phosphorylcholine-co-*n*-butyl methacrylate), Polym. J. 31 (1999) 1231–1236.
[45] K. Konno, J. Watanabe, K. Ishihara, Conjugation of enzymes on polymer nanoparticles covered with phosphorylcholine groups, Biomacromolecules 5 (2004) 342–347.
[46] J. Watanabe, K. Ishihara, Single step diagnosis system using the FRET phenomenon induced by antibody-immobilized phosphorylcholine group-covered polymer nanoparticles, Sens. Actuat. B: Chem. 129 (2008) 87–93.
[47] J. Watanabe, K. Ishihara, Sequential enzymatic reactions and stability of biomolecules immobilized onto phospholipid polymer nanoparticles, Biomacromolecules 7 (2006) 171–175.
[48] T. Ito, J. Watanabe, M. Takai, T. Konno, Y. Iwasaki, K. Ishihara, Dual mode bioreactions on polymer nanoparticles covered with phosphorylcholine group, Colloids Surf. B: Biointerfaces 50 (2006) 55–60.
[49] Y. Goto, R. Matsuno, T. Konno, M. Takai, K. Ishihara, Polymer nanoparticles covered with phosphorylcholine groups and immobilized with antibody for high-affinity separation of proteins, Biomacromolecules 9 (2008) 828–833.
[50] A.A. Garcia, Bioseparation Process Science, Blackwell Science Inc., Cambridge, MA, 1999.
[51] A.M. Smith, H. Duan, A.M. Mohs, S. Ni, Bioconjugated quantum dots for in vivo molecular and cellular imaging, Adv. Drug Deliv. Rev. 60 (2008) 1226–1240.
[52] T. Jamiesona, R. Bakhshia, D. Petrovaa, R. Pococka, M. Imanib, A.M. Seifaliana, Biological applications of quantum dots, Biomaterials 28 (2007) 4717–4732.
[53] A.F.E. Hezinger, J. Teßmar, A. Gopferich, Polymer coating of quantum dots—a powerful tool toward diagnostics and sensorics, Eur. J. Pharm. Biopharm. 68 (2008) 138–152.
[54] Y. Goto, R. Matsuno, T. Konno, M. Takai, K. Ishihara, Artificial cell membrane-covered nanoparticles embedding quantum dots as stable and highly sensitive fluorescence bioimaging probes, Biomacromolecules 9 (2008) 3252–3257.
[55] X. Wu, H. Liu, J. Liu, K.N. Haley, J.A. Treadway, J.P. Larson, N. Ge, F. Peale, M.P. Bruchez, Immunofluorescent labeling of cancer marker Her2 and other cellular targets with semiconductor quantum dots, Nat. Biotechnol. 21 (2003) 41–46.
[56] B. Dubertret, P. Skourides, D.J. Norris, V. Noireaux, A.H. Brivanlou, A. Libchanber, In vivo imaging of quantum dots encapsulated in phospholipid micelles, Science 298 (2002) 1759–1762.
[57] T. Moro, Y. Takatori, K. Ishihara, T. Konno, Y. Takigawa, T. Matsushita, U.I. Chung, K. Nakamura, H. Kawaguchi, Surface grafting of artificial joints with a biocompatible polymer for preventing periprosthetic osteolysis, Nat. Mater. 3 (2004) 829–836.
[58] I.A. Khalil, K. Kogure, S. Futaki, S. Hama, H. Akita, M. Ueno, H. Kishida, M. Kudoh, Y. Mishima, K. Kataoka, M. Yamada, H. Harashima, Octaarginine-modified multifunctional envelope-type nanoparticles for gene delivery, Gene Ther. 14 (2007) 682–689.
[59] A. El-Sayed, I.A. Khalil, K. Kogure, S. Futaki, H. Harashima, Octaarginine- and octalysine-modified nanoparticles have different modes of endosomal escape, J. Biol. Chem. 283 (2008) 23450–23610.

Reactive & Functional Polymers 71 (2011) 350–355

Contents lists available at ScienceDirect

Reactive & Functional Polymers

journal homepage: www.elsevier.com/locate/react

Adhesion force of proteins against hydrophilic polymer brush surfaces

Yuuki Inoue [a], Tomoaki Nakanishi [a], Kazuhiko Ishihara [a,b,c,*]

[a] Department of Materials Engineering, School of Engineering, The University of Tokyo, 7-3-1, Hongo, Bunkyo-ku, Tokyo 113-8656, Japan
[b] Department of Bioengineering, School of Engineering, The University of Tokyo, 7-3-1, Hongo, Bunkyo-ku, Tokyo 113-8656, Japan
[c] Core Research for Evolutional Science and Technology (CREST), Japan Science and Technology Agency (JST), 5 Sanban-cho, Chiyoda-ku, Tokyo 102-0075, Japan

ARTICLE INFO

Article history:
Available online 19 November 2010

Keywords:
Polymer brush layer
Surface-initiated atom transfer radical polymerization
Surface modification
Atomic force microscopy
Adhesion force of proteins

ABSTRACT

Protein adsorption occurs on the surface of biomaterials when they are exposed to physiological environments. The protein adsorption layer induces severe biological responses, including cellular reactions. Protein adsorption layers are formed mainly by two distinct processes: monolayer adsorption of proteins on the surface and a subsequent additional adsorption on the first layer to form a multilayer. Therefore, evaluating the first protein adsorption is important to understand the biological responses on the surface of materials. In this study, we applied the atomic force microscopic (AFM) technique to directly measure the adhesion force of proteins against the surface (i.e., the interaction between proteins and surface). We also prepared hydrophilic polymer brush surfaces with well-known high repellency against protein adsorption through surface-initiated atom transfer radical polymerization. Polymer brush layers have a well-defined surface structure; therefore, it could be a good model for clarifying the relationship between the surface structure and protein adsorption behavior. The influence of chemical structure of monomer unit and thickness of polymer brush layers on the adhesion force of proteins was discussed here, while that of graft density was not discussed. The adhesion force of bovine serum albumin (BSA) immobilized on an AFM cantilever against the thin polymer brush surfaces differed from the chemical structures of the monomer unit. The adhesion force of BSA decreased with increasing thickness of the polymer brush layer, and there was little difference in the adhesion force of BSA against the thick polymer brush surfaces regardless of the chemical structure of the monomer unit. The results demonstrate that the thickness of the polymer brush layer would be an important parameter that reduced the interaction between proteins and surfaces compared with the chemical structure of the monomer unit.

1. Introduction

Protein adsorption on the surface of materials is an important factor that determines subsequent biological responses, including cellular reactions. In particular, nonspecific protein adsorption and deposition on the surface may result in several serious problems, such as immunoreaction, blood coagulation, and inflammatory reaction [1]. A variety of polymeric biomaterial surface designs have been proposed to suppress nonspecific protein adsorption, such as induction of higher polymer chain mobility by poly(ethylene oxide) [2–4] and construction of artificial cell membrane structures by using phospholipid polymers [5–8]. In recent years, surface-initiated grafting of functional monomers to obtain a polymer brush structure has attracted much attention in biomedical research because it restricts protein adsorption to 5 ng/cm^2, which is approximately 300 times less than the protein adsorption mass on conventional materials, including polystyrene for cell culture, glass, etc. [9–18]. On the other hand, the mechanism for obtaining high repellency against protein adsorption in the polymer brush structure is still unclear.

Protein adsorption on the surface in physiological environments involves two stages. First, proteins directly adsorb on the surface of the materials through several kinds of intermolecular interactions between proteins and the surface, occurring under aqueous conditions, which form a single layer of adsorbed proteins. Second, proteins interact with the preadsorbed protein monolayer, the conformation of which would be changed by the interaction with the surface of materials. In this regard, it is important to characterize the direct interactions between proteins and the surface. Measurement of direct interaction is distinctly different from quantification of the protein adsorption mass on the surface of a material; the latter merely estimates the amount of whole proteins adsorbed on the multilayer. Atomic force microscopy (AFM) allows the quantification of the specific force between the biomolecules immobilized on a given surface and probes, such as antigen–antibody [19] and ligand–receptor [20]. In addition, the direct force of nonspecific interactions between proteins and several kinds of

* Corresponding author at: Department of Materials Engineering, School of Engineering, The University of Tokyo, 7-3-1, Hongo, Bunkyo-ku, Tokyo 113-8656, Japan. Tel.: +81 3 5841 7124; fax: +81 3 5841 8647.
E-mail address: ishihara@mpc.t.u-tokyo.ac.jp (K. Ishihara).

1381-5148/$ - see front matter © 2010 Elsevier Ltd. All rights reserved.
doi:10.1016/j.reactfunctpolym.2010.11.017

self-assembled monolayers [21] and grafted polymer surfaces [22] has also been evaluated. In all previous studies, the forces in the order of a few piconewtons were detected, and the phenomena that occurred in the microenvironment of the biomaterial surface were manifested. To our knowledge, no research has been conducted on the direct measurement of the adhesion force of proteins against the polymer brush layers. Because the polymer brush layers have a well-defined surface structure, analysis of the adhesion force of proteins against them could provide a novel understanding of the behavior of protein adsorption on a biomaterial surface.

In this study, we prepared poly(2-methacryloyloxyethyl phosphorylcholine) (PMPC), poly(oligo(ethylene glycol) monomethacrylate) (POEGMA), and poly(2-hydroxyethyl methacrylate) (PHEMA) brush layers on silicon wafers by using the surface-initiated atom transfer radical polymerization (SI-ATRP) method with a sacrificial initiator. To obtain information on the polymer brush layer, we characterized its surface structure and properties by using AFM, X-ray photoelectron spectroscopy (XPS), spectroscopic ellipsometry, and static contact angle measurement under dry and wet conditions. Then, the adhesion force of proteins against these polymer brush layers was quantified using an AFM with a protein-immobilized cantilever. This study analyzed the effect of layer thickness and monomer moiety of well-characterized polymer brush structures on the adhesion force of proteins. The results demonstrate that the thickness of the polymer brush layer has a relatively larger influence on the reduction of the adhesion force of proteins than the chemical structure of the polymer brush layer.

2. Experimental

2.1. Materials

MPC was synthesized and purified using a previously reported method [5]. OEGMA with a repeating number (n) of ethylene glycols of 4, HEMA, and bovine serum albumin (BSA) were purchased from Sigma–Aldrich Co. (St. Louis, MO, USA). Copper (I) bromide (CuBr), 2,2′-bipyridyl (bpy), and ethyl-2-bromoisobutyrate (EBIB) were purchased from Sigma–Aldrich Co. and were directly used as received. Triethylamine (TEA) was purchased from Kanto Chemical Co. (Tokyo, Japan) and used after distillation at 95 °C. All other reagents and solvents of extra-pure grade were commercially available and were used as purchased. Silicon wafers were purchased from Furuuchi Chemical Co. (Tokyo, Japan); the surface of the silicon wafers was coated with approximately 10-nm-thick SiO_2 layers. High-purity grade oxygen and argon gases were used.

2.2. Preparation of initiator-immobilized substrate

To prepare the homogeneous monolayer of the initiator on the silicon wafers, a surface-immobilizing initiator, 3-(2-bromoisobutyryl)decyl dimethylchlorosilane (BrC10DMCS), was synthesized as previously described [23]. The silicon wafers, which were adequately rinsed by sonication with hexane, ethanol, and acetone, and etched by using oxygen plasma (PR500; Yamato Scientific Co. Ltd., Tokyo, Japan), were immersed in a 50 mmol/L solution of BrC10DMCS in toluene for 72 h under inert conditions in the presence of TEA as a catalyst and acid scavenger. The wafers were removed from the solution, rinsed with toluene and methanol, and dried *in vacuo* until they were used for graft polymerization.

2.3. Preparation of polymer brush layers

MPC, OEGMA, and HEMA were graft polymerized from the BrC10DMCS-immobilized substrate by using SI-ATRP as follows [14]. CuBr, bpy, and each monomer in a particular molar ratio were placed in a glass tube and dehydrated; thereafter, degassed solvents were added into the glass tube. The following solvents were used: methanol for MPC and HEMA at monomer concentrations of 0.56 mol/L and 2.0 mol/L, respectively, and a mixture of methanol and tetrahydrofuran (THF) (1:1 by volume) for OEGMA at a concentration of 0.50 mol/L. Argon was bubbled into each monomer solution at room temperature for 10 min. The BrC10DMCS-immobilized substrate was then immersed in the solution, and EBIB was simultaneously added as the free initiator at a defined concentration. After the glass tubes were sealed, polymerization was performed at room temperature with stirring. After 24 h, the substrate was removed from the polymerization solution, rinsed, and purified with ultrasonication for 5 min in methanol and dried in a nitrogen stream. We prepared polymer brush layers for each type of monomer at [Monomer]/[Initiator] ratios of 10, 20, and 50; the ratio was represented after the abbreviation of the polymer name (i.e., PMPC10, POEGMA10, and PHEMA10). The chemical structures of the monomer units used for the synthesis of PMPC, POEGMA, and PHEMA brush layers are shown in Fig. 1.

The conversion of monomers in different polymerization solutions was determined using nuclear magnetic resonance spectroscopy (^{1}H NMR; JEOL, Tokyo, Japan). The molecular weights and polydispersities of free polymers in the reaction solutions were determined through gel permeation chromatography (GPC) using a methanol/water mixture (70:30) containing 10 mmol/L lithium bromide as an eluent and poly(ethylene glycol) as standard.

2.4. Surface characterization

The composition of surface elements was determined using an XPS (AXIS-Hsi; Shimadzu/Kratos, Kyoto, Japan) with a magnesium anode nonmonochromatic source. The samples were completely dried *in vacuo* before the measurement. High-resolution scans for C_{1s}, O_{1s}, N_{1s}, and P_{2p} were acquired at a takeoff angle of 90° for the photoelectrons. All binding energies were referred to the C_{1s} peak at 285.0 eV.

The thickness of the grafted polymer layers present on the BrC10DMCS-immobilized substrates was determined under dry conditions by using a spectroscopic ellipsometer (J.A. Woollam

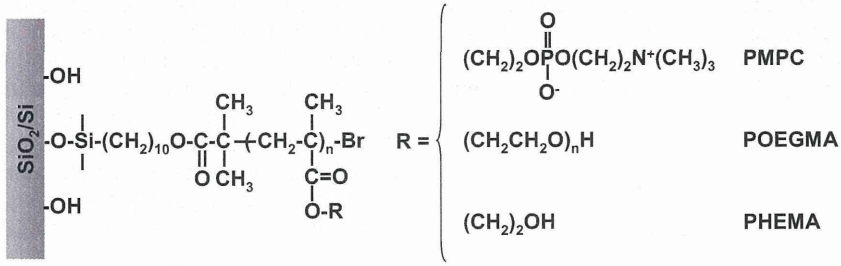

Fig. 1. Chemical structures of the monomer units used for the synthesis of polymer brush layers on the silicon wafers.

Co. Inc., Tokyo, Japan). The BrC10DMCS-immobilized substrate and each polymer brush layer were measured at an incident angle of 70° in the visible region. The thickness of the grafted polymer layers was determined using the Cauchy layer model with an assumed refractive index of 1.49 at 632.8 nm. The graft density (σ [chains/nm^2]) was calculated from the ellipsometric thickness determined for each grafted polymer layer by using the equation:

$$\sigma = h\rho N_A/M_n, \quad (1)$$

where h is the ellipsometric thickness (nm), ρ is the density of each dry polymer (1.30 g/cm^3 for PMPC [13] and 1.15 g/cm^3 for POEGMA and PHEMA [9]), N_A is Avogadro's number, and M_n is the absolute molecular weight of the polymer chains on the surface, which was estimated from the polymerization degree determined using the ^{1}H NMR spectrum of each free polymer. This estimation has been validated for polystyrene and poly(methyl methacrylate (MMA)) [24,25].

The surface morphology of the polymer brush layers under aqueous conditions was observed using an AFM (Nanoscope IIIa; Nihon Veeco, Tokyo, Japan) operated in the tapping mode. The measurements were performed using a standard cantilever at a scan rate of 1.0 Hz, and a scan size of 1 μm × 1 μm. Before the measurements, the samples were immersed in aqueous medium for 24 h. The root mean square (RMS) of the surface roughness was calculated from the roughness profiles.

The static water contact angles under dry conditions and air contact angles in an aqueous medium by captive bubble methods were measured using a goniometer (CA-W; Kyowa Interface Science Co., Tokyo, Japan) at room temperature. The samples were completely dried *in vacuo* before the measurement of static water contact angle. Water droplets of 3 μL volume were brought in contact with the substrates. On the other hand, the samples were immersed in water for 24 h before the measurement of air contact angle. Air bubbles of 5 μL volume were brought in contact with the substrates. All contact angles were directly measured from the photographic images. We show the supplementary angle (180°–θ) of the static air bubble contact angle in aqueous conditions (θ) for easy comparison with static water contact angles in dry conditions. Data were collected for more than three positions for each sample.

2.5. Protein adhesion force measurement

BSA was covalently immobilized on an AFM cantilever through the condensation reaction between the amino groups in the protein and the carboxyl groups on the AFM cantilever [21]. Commercially available 200-μm-long V-shaped Si_3N_4 cantilevers (OTR8; Veeco NanoProbe Tips) with an announced spring constant of 0.15 N/m were used. Gold film was prepared on the Si_3N_4 cantilever by using plasma spattering with 3.0 nm adhesion layer of Cr followed by 27 nm of Au. The oxygen-plasma-treated Au-coated cantilever was immersed in 1.0 mmol/L solution of 11-mercaptoundecanoic acid in ethanol for 1 h to form a carboxyl group-terminated self-assembled monolayer (COOH-SAM). After rinsing with ethanol and water, the cantilever was immersed in water solution of 1-ethyl-3-(3-dimethylaminopropyl) carbodiimide hydrochloride (0.1 mol/L) and *N*-hydroxysuccinimide (0.05 mol/L) for 30 min. The cantilever was washed with water and immediately immersed in phosphate-buffered saline (PBS) solution of BSA (1 mg/mL) for 1.5 h at 37 °C. The BSA-immobilized cantilever was kept in PBS at 4 °C until use. The immobilization of proteins on the cantilever was confirmed using quartz crystal microbalance with dissipation (QCM-D) and XPS measurements by using a QCM gold sensor and gold-evaporated silicon wafer instead of the cantilever, respectively.

The adhesion force between BSA immobilized on the cantilever and BrC10DMCS-immobilized and polymer brush layers in PBS solution was evaluated from the approaching and retracting trace of force-versus-distance (f–d) curve at room temperature. The shift value of deflection in the retract trace of the f–d curves from the bottom of the retrace line corresponds to the adhesion force. In each measurement, more than 100 of the approaching/retracting f–d curves were collected, and the average value was defined as the adhesion force between BSA and substrates.

All measurements were repeated at least three times.

3. Results and discussion

3.1. Surface structure of polymer-grafted substrates

In this study, three kinds of polymer brush layers, PMPC, POEGMA, and PHEMA, were prepared on the BrC10DMCS-immobilized substrate using SI-ATRP with a free initiator. The semilogarithmic plot of monomer concentrations versus polymerization time, and the plot of molecular weight of the free polymers versus monomer conversion, remained linear during graft polymerization of the respective monomers from the BrC10DMCS-immobilized substrate, indicating the successful polymerization in the ATRP process [14]. At the end of the 24-h polymerization, the polydispersity of the respective free polymers was quite low (<1.3). Husseman et al. [24] and Yamamoto et al. [25] reported similarities in the properties of grafted polymers and polymers that formed in solution. Taking the reported results into account, the polymer brush layers prepared in this study would grow uniformly on the silicon wafer.

The surface elements of the polymer-grafted substrates were analyzed using the XPS spectra. The peaks of the carbon atom region (C_{1s}) at 285.0, 286.5, and 289.0 eV in all substrates corresponded to the neutral carbon, ether bond, and ester bond in the methacrylate group, respectively [14]. We detected the peaks of the phosphorus atom region (P_{2p}) at 133.0 eV, which corresponded to the phosphate group, and of the nitrogen atom region (N_{1s}) at 403.0 eV, which corresponded to the protonated ammonium group [14,26]. These peaks were specific to the phosphorylcholine group of the MPC unit. Thus, XPS analysis confirmed the identities of the monomer elements of each polymer chain on the surface of the silicon wafers.

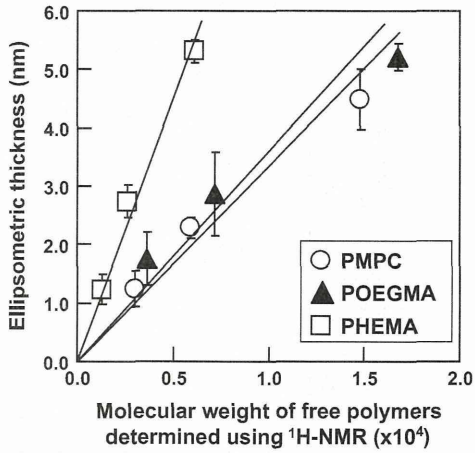

Fig. 2. Relationship between the absolute molecular weight of the polymer chains and the ellipsometric thickness of the grafted poly(2-methacryloyloxyethyl phosphorylcholine) (PMPC) layer (open circles), grafted poly(oligo(ethylene glycol) monomethacrylate) (POEGMA) layer (closed triangles), and grafted poly(2-hydroxyethyl methacrylate) (PHEMA) layer (open squares), under dry conditions.